FULL PAPERS

Magnetic Resonance in Medicine 61:1279–1285 (2009)

MR Spectroscopy of the Human Brain With Enhanced Signal Intensity at Ultrashort Echo Times on a Clinical Platform at 3T and 7T

Ralf Mekle,[1,2*] Vladimír Mlynárik,[1] Giulio Gambarota,[1] Martin Hergt,[3] Gunnar Krueger,[3] and Rolf Gruetter[1,2,4]

Recently, the spin-echo full-intensity acquired localized (SPECIAL) spectroscopy technique was proposed to unite the advantages of short TEs on the order of milliseconds (ms) with full sensitivity and applied to in vivo rat brain. In the present study, SPECIAL was adapted and optimized for use on a clinical platform at 3T and 7T by combining interleaved water suppression (WS) and outer volume saturation (OVS), optimized sequence timing, and improved shimming using FASTMAP. High-quality single voxel spectra of human brain were acquired at TEs below or equal to 6 ms on a clinical 3T and 7T system for six volunteers. Narrow linewidths (6.6 ± 0.6 Hz at 3T and 12.1 ± 1.0 Hz at 7T for water) and the high signal-to-noise ratio (SNR) of the artifact-free spectra enabled the quantification of a neurochemical profile consisting of 18 metabolites with Cramér-Rao lower bounds (CRLBs) below 20% at both field strengths. The enhanced sensitivity and increased spectral resolution at 7T compared to 3T allowed a two-fold reduction in scan time, an increased precision of quantification for 12 metabolites, and the additional quantification of lactate with CRLB below 20%. Improved sensitivity at 7T was also demonstrated by a 1.7-fold increase in average SNR (= peak height/root mean square [RMS]-of-noise) per unit-time. Magn Reson Med 61:1279–1285, 2009.

Key words: human brain; proton magnetic resonance spectroscopy; high magnetic field; short echo time; 3T; 7T

Stimulated-echo acquisition mode (STEAM) (1) or point-resolved spectroscopy (PRESS) (2) are the major methods used for localized proton magnetic resonance spectroscopy (MRS). As STEAM suffers a two-fold signal loss compared to PRESS, but allows shorter echo times (TEs), it is highly desirable to combine the short TE achievable with STEAM with the full signal intensity provided by PRESS. In general, short echo times below 20 ms offer the benefits of reduced signal decay due to T_2 relaxation and J-evolution of coupled spin systems. This in turn allows a more precise quantification of metabolites including those with short T_2 relaxation times. In addition, signal contributions from macromolecules that generally exhibit short T_2s can be analyzed in short TE spectra to provide insight into specific diseases (3). Short echo times are more easily achievable with STEAM because of the lower peak radiofrequency (RF) pulse power requirements for 90° compared to 180° pulses. This is especially important for studies in humans, where the available peak RF power is limited. The STEAM technique was extensively used in previous studies to acquire human brain spectra at field strengths of 1.5T, 3T, 4T, and 7T using TE = 5 ms (4) and 6 ms (5), 6.8 ms (6), 4 ms (7), and 6 ms (8), respectively.

On the other hand, it is advantageous to acquire the signal of the full magnetization using spin-echo (SE)-based methods, such as PRESS. For the aforementioned reasons, only few studies report results acquired at short TE. Reducing crusher gradients and using short RF pulses in one approach, or utilizing a dedicated transmit/receive head coil at 3T in pediatric patients in another approach, enabled PRESS acquisitions of in vivo human single-voxel spectroscopy (SVS) data at TE ≈ 10 ms (9,10). Using the proton echo-planar spectroscopic imaging technique, a TE of 15 ms was reported in MR spectroscopic imaging (MRSI) at 3T and 4T (11).

The advantages of short TEs on the order of milliseconds (ms) were recently combined with full signal intensity achieved with SE-based scans using the SE full intensity acquired localized (SPECIAL) spectroscopy technique and applied to in vivo rat brain (12). The sequence benefits from RF coils producing strong B_1 fields and combines interleaved water suppression (WS) and outer volume saturation (OVS), optimized sequence timing, and improved localized shimming. Moreover, the application of SPECIAL at high B_0 fields (≥3T) sought to take advantage of the corresponding increased sensitivity and increased spectral resolution, particularly at 7T, where so far only few in vivo human MRS studies at short TE using STEAM have been conducted on experimental scanners (8).

Therefore, the aim of this study was to implement and optimize SPECIAL on a clinical platform at 3T and at 7T and to obtain high-quality single-voxel spectra of the hu-

[1]Laboratory for Functional and Metabolic Imaging (LIFMET), Ecole Polytechnique Federale de Lausanne, Lausanne (EPFL), Switzerland.

[2]Department of Radiology, University of Lausanne, Lausanne, Switzerland.

[3]Advanced Clinical Imaging Technology, Siemens Medical Solutions–Centre d'Imagerie BioMedicale (CIBM), Lausanne, Switzerland.

[4]Department of Radiology, University of Geneva, Geneva, Switzerland.

Grant sponsors: Centre d'Imagerie BioMédicale (CIBM) of the University of Lausanne (UNIL), University of Geneva (UNIGE), Hôpitaux Universitaires de Genève (HUG), Centre Hospitalier Universitaire Vaudois (CHUV), Ecole Polytechnique Federale de Lausanne (EPFL); Leenaards Foundation; Jeantet Foundation.

*Correspondence to: Ralf Mekle, Ph.D., Centre d'Imagerie BioMedicale (CIBM), Ecole Polytechnique Federale de Lausanne (EPFL), EPFL SB IPMC LIFMET, CH F 0 572 (Batiment CH), Station 6, 1015 Lausanne, Switzerland. E-mail: ralf.mekle@epfl.ch

Received 12 September 2008 ; revised 22 December 2008; accepted 23 December 2008.

DOI 10.1002/mrm.21961

Published online 24 March 2009 in Wiley InterScience (www.interscience.wiley.com).

man brain at ultrashort TEs (≤10 ms). In addition, an initial comparison of the results obtained at the two different field strengths was performed in terms of signal-to-noise ratio (SNR) and reliability of metabolite quantification.

MATERIALS AND METHODS

All scans were performed on a 90-cm bore clinical 3T (Magnetom Trio, a Tim System, Syngo MR VB15) scanner equipped with a whole-body gradient coil (40 mT/m, 200 mT/[m·ms]) and an actively-shielded 7T (Tim System, Syngo MR VB15) human head system of 68-cm bore with a head gradient coil (60 mT/m, 330 mT/[m·ms]) (Siemens Medical Solutions, Erlangen, Germany). On both systems, a quadrature transmit (Tx)/receive (Rx) surface RF coil consisting of two decoupled single-turn coils of 13-cm-diameter was used (13). At 3T, data were also acquired using a transverse electromagnetic (TEM) volume coil (14) (MR Instruments, Inc., Minneapolis, MN, USA).

Pulse Sequence

SPECIAL (12) combines an one-dimensional (1D) image-selected in vivo spectroscopy (ISIS) (15) approach with a slice-selective SE sequence (see Fig. 1). Full localization was accomplished by using an add-subtract scheme, where the signal was added in odd scans and subtracted in even scans corresponding to the application of an adiabatic inversion pulse. The implementation of SPECIAL was adapted and optimized for a clinical platform as follows: due to the reduced peak RF power and gradient strengths, all settings and durations of RF pulses and gradients were readjusted and calibrated. Water signal suppression was achieved using variable-pulse power and optimized relaxation delays (VAPOR) (16) plus an additional Gaussian WS pulse that was executed after the adiabatic inversion pulse (see Fig. 1). The bandwidth of the Gaussian WS pulses was set to 45 Hz at 3T and to 60 Hz at 7T to account for different linewidths and chemical shift dispersions at the two B_0 fields. The VAPOR WS scheme was interleaved with multiple blocks of OVS to reduce contaminating signals originating from extracranial lipids. Timing and delays of this interleaved sequence module were separately adjusted for the two field strengths based on approaches described in (7). Hyperbolic-secant RF pulses with 5.0-ms duration, an 8.4 kHz bandwidth, a peak B_1 amplitude ($\gamma/2\pi \cdot B_{1max}$) of 0.75 kHz, and a nominal flip angle of 90° were used for OVS to minimize chemical shift artifacts. In addition, each hyperbolic-secant RF pulse was also executed with a RF transmitter voltage that was increased by a factor of the square root of 2 to improve the effectiveness of the OVS in the presence of a spatially inhomogeneous B_1 field. For inversion, a hyperbolic-secant RF pulse with T_{Pulse} = 5.12 ms, BW_{RF} = 2.1 kHz, and ($\gamma/2\pi \cdot B_{1max}$) = 0.75 kHz was employed. Large B_1 peak amplitudes and the use of an asymmetric RF excitation pulse in the SPECIAL method allowed ultrashort echo times (TE_{min} = 3.5 ms at 3T and 5.5 ms at 7T). To obtain a typical TE = 6 ms, T_{Pulse} = 1.28 ms with BW_{RF} = 5.3 kHz and ($\gamma/2\pi \cdot B_{1max}$) = 1.3 kHz and T_{Pulse} = 3.2 ms with BW_{RF} = 1.8 kHz and ($\gamma/2\pi \cdot B_{1max}$) = 1.7 kHz were used for the asymmetric RF excitation (16) and for the symmetric refocusing pulse introduced by Mao et al. (17), respectively. Spoiler gradients were inserted to dephase any potential transverse magnetization.

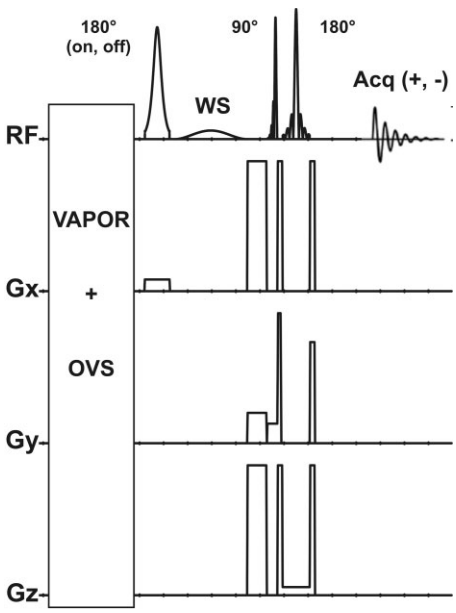

FIG. 1. Schematic of the SPECIAL pulse sequence. The first 180° pulse is adiabatic and is applied in alternate scans, together with alternating the phase of the receiver. WS represents an additional water saturation pulse.

Data Acquisition and Metabolite Quantification

For data acquisition, a volume-of-interest (VOI) in the occipital lobe was selected using T_1-weighted (3T) or T_2^*-weighted (7T) gradient echo (GRE) scout images. Each volunteer was scanned on both systems, and placement of the VOI was the same based on anatomical landmarks for both scans and also across volunteers. In addition to a localized calibration of RF transmitter voltages for the selected VOI, flip angles of the WS pulses were optimized for each individual subject, and position and size of the OVS bands were slightly adapted interactively according to voxel location. First- and second-order shims were adjusted using a fully adiabatic version of FASTMAP/FASTESTMAP (18,19). After concluding all adjustment procedures, ^{1}H single-volume acquisitions of the human brain were performed using the following scan parameters: VOI = 20 × 20 × 20 mm^3, TR/TE = 4000 ms/6 ms, spectral width = 2 kHz (3T) or 4 kHz (7T), number of averages (NA) = 128 (3T) or 64 (7T), vector size = 2048, delta of excitation frequency (δf_{exc}) = –2.3 ppm (i.e., the reference frequency used for calculating offsets of slice-elective RF pulses was shifted 2.3 ppm upfield from the water resonance). Data were acquired for N = 6 volunteers aged 22–26 years. Spectral quality was such that neither eddy current postprocessing, nor water removal, nor baseline correction was necessary or applied. The spectra were quantitatively analyzed using LCModel (20) with basis sets for the two different field strengths created by quantum mechanics simulations. For the 3T data, a set of macro-

molecules was provided by LCModel, whereas for the 7T spectra an experimentally acquired set of macromolecules was used. The LCModel analysis was carried out on spectra for chemical shifts in the range of 0.2 to 4.2 ppm. Results from metabolite quantification for 3T and 7T data were compared, and differences were statistically evaluated using the *t*-test.

RESULTS

Ultrashort TE ^{1}H SVS data from the human brain were acquired at 3T (Fig. 2) and at 7T (Fig. 3). Peaks of glutamine (Gln) and glutamate (Glu) were clearly resolved at both fields. Baseline distortions that might be visible in ultrashort TE spectra were not observed. Comparing the two spectra in Fig. 2 and Fig. 3, it is noted that the increased spectral resolution at 7T due to increased chemical shift dispersion and generally simplified J-coupling patterns yields an increased number of resolved spectral features, such as the doublet of aspartate (Asp) at 2.80 ppm and the triplet of γ-aminobutric acid (GABA) at 2.28 ppm, and an improved separation of spectral lines of individual metabolites, such as Gln and Glu or Scyllo-inositol (Scyllo) and taurine (Tau). Reproducibly across volunteers, the obtained data showed excellent WS, especially at 7T, as seen in Fig. 2 and Fig. 3. In all cases, the residual signal of water was smaller than the singlet of N-acetylaspartate (NAA) at 2.01 ppm. In addition, the lipid contamination was sufficiently suppressed by the application of OVS illustrated by the consistently artifact-free region of the spectra around 1.3 ppm (Figs. 2 and 3). Localized shimming using FASTMAP/FASTESTMAP resulted in water linewidths measured as full-linewidth at half-maximum ($FWHM_{H2O}$) ranging from 6.0 to 7.5 Hz with a mean $FWHM_{H2O} = 6.6 \pm 0.6$ Hz in gray matter (GM)-rich regions of the occipital lobe at 3T. At 7T, $FWHM_{H20}$ in the range of

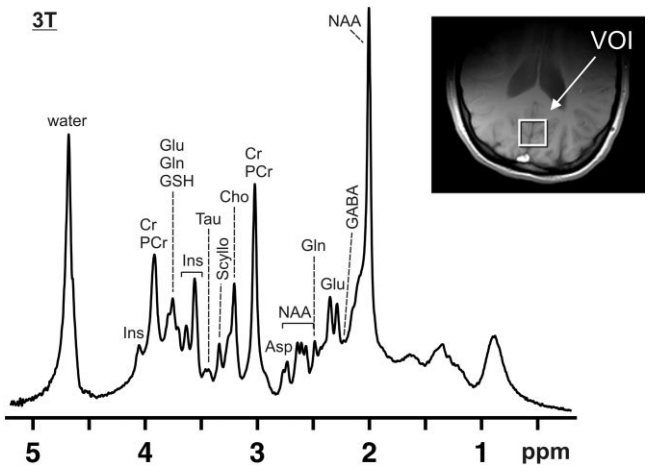

FIG. 2. ^{1}H NMR spectrum from a GM-rich VOI = 20 × 20 × 20 mm^3 in the occipital lobe of a volunteer acquired with an optimized SPECIAL acquisition scheme at 3T. TR/TE = 4000 ms/6 ms, NA = 128, and BW = 2 kHz. Data processing consisted of zero-filling up to 8-k data points, 1 Hz Gaussian weighting of the free induction decay (FID), Fourier transformation, and phase correction. Note the excellent data quality of the artifact-free spectrum. Inset: transverse T_1-weighted GRE image with the location of the VOI.

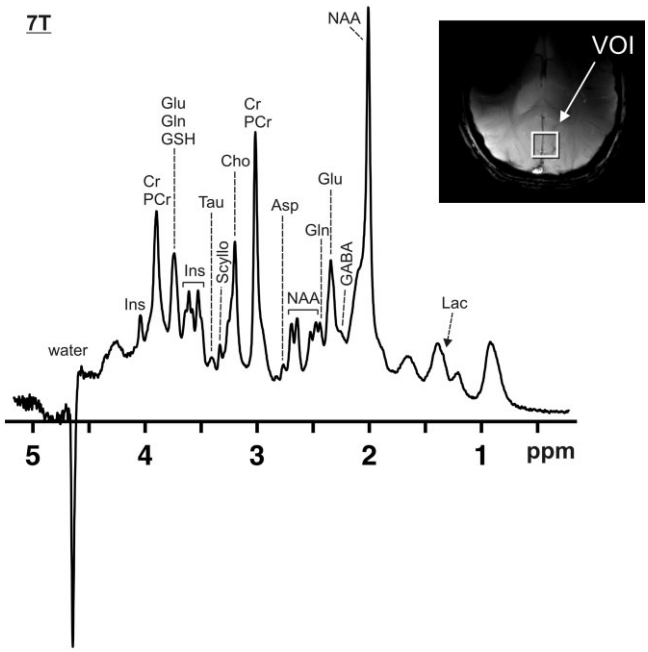

FIG. 3. ^{1}H NMR spectrum from the occipital lobe of the same volunteer as shown in Fig. 2 acquired with SPECIAL at 7T using the same scan parameters, except for NA = 64 and BW = 4 kHz. Data processing was the same as for Fig. 2, except for a 2-Hz Gaussian weighting of the faster-decaying FID at 7T. Comparing the spectrum with the data presented in Fig. 2, the increased spectral resolution at the higher field becomes apparent. Inset: transverse T_2^*-weighted GRE image with the location of the VOI.

10.9 to 13.5 Hz with a mean $FWHM_{H20} = 12.1 \pm 1.0$ Hz were obtained in similar voxel locations. Using the SPECIAL acquisition scheme at ultrashort TEs resulted in a high SNR. The ultrashort TEs reduced signal attenuation due to T_2 relaxation as well as modulation of J-coupled multiplets. The average SNR, i.e., the maximum peak-height, which in this case corresponded to the height of the NAA peak at 2.01 ppm, divided by the root mean square (RMS) of residual (unfitted) noise, calculated by LCModel analysis was 64.8 ± 3.1 at 3T and 76.5 ± 5.2 at 7T. Considering that the spectra at 7T were acquired in one-half the scan time, the ratio of the average SNR per unit-time between the two field strengths was calculated to be 1.7.

An example for data acquired with a TEM volume coil from a VOI in parietal white matter is presented in Fig. 4. In this case, $FWHM_{H20}$ was 6.2 Hz, and a SNR of 48 was calculated. Spectral quality was similar to the one of the data shown in Fig. 2 including the absence of lipid contaminations. With respect to data quality this example was representative for several different acquisitions performed with the TEM volume coil.

Metabolite Quantification

Figure 5 shows the corresponding fitted curves using LCModel for the ^{1}H spectra displayed in Fig. 2 and in Fig. 3. At both field strengths, analysis using LCModel yielded excellent fits of the spectra illustrated by the small residuals included directly below the respective LCModel fit of

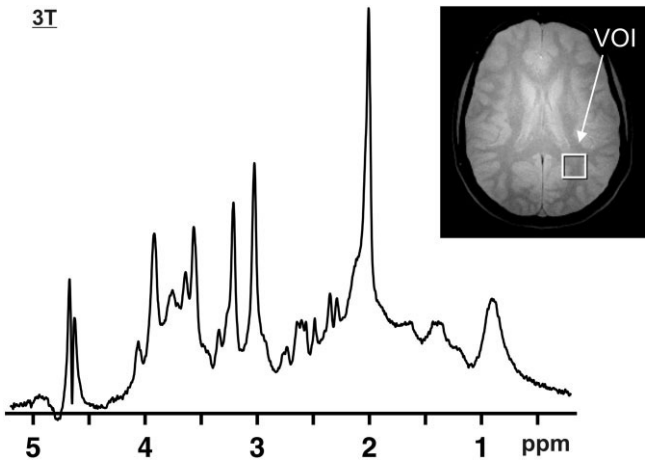

FIG. 4. ^{1}H NMR spectrum from a VOI = 20 × 20 × 20 mm^3 in the parietal white matter of a volunteer acquired with an optimized SPECIAL acquisition scheme at 3T using a TEM volume head coil. TR/TE = 2000 ms/6 ms, NA = 256, and BW = 2 kHz. Data processing was the same as in Fig. 2. Data quality was similar to the one of the spectra shown in Fig. 2, except for a slightly reduced SNR as is expected from the use of a volume coil. Inset: transverse T_2^*-weighted GRE image with the location of the VOI.

each spectrum in Fig. 5a and b. Metabolite linewidths determined from the singlet of creatine (Cr) at 3.03 ppm were estimated as 4.3 ± 0.2 Hz and 8.5 ± 0.9 Hz at 3T and 7T, respectively. Resulting absolute metabolite concentrations together with their respective Cramér-Rao lower bounds (CRLBs) were compared for 18 metabolites at both fields, which had average CRLBs below 20% (Table 1; not including lactate (Lac) and glucose (Glc)). The CRLB averaged over all these metabolites was 35% lower at 7T than at 3T, which was significant ($P < 0.015$). For 12 metabolites the CRLB was on average reduced by 38%, and for six metabolites it was approximately equal. A substantial improvement in CRLB was observed at 7T for Gln, Tau, and Gln+Glu. Moreover, Lac was additionally quantified with CRLB below 20% at the higher field, yielding a concentration of 0.7 ± 0.1 mmol/kg with CRLB of 9 ± 1.6%. In contrast, the concentration of Glc was more reliably determined at 3T as 1.4 ± 0.3 mmol/kg with a CRLB of 14 ± 2.7%. The average difference between metabolite concentrations determined at both fields was 2%, which was not significant ($P > 0.22$). Differences in concentrations for the metabolites shown in Table 1 were within 15%, except for phosphocreatine (PCr), GABA, Gln, and Scyllo.

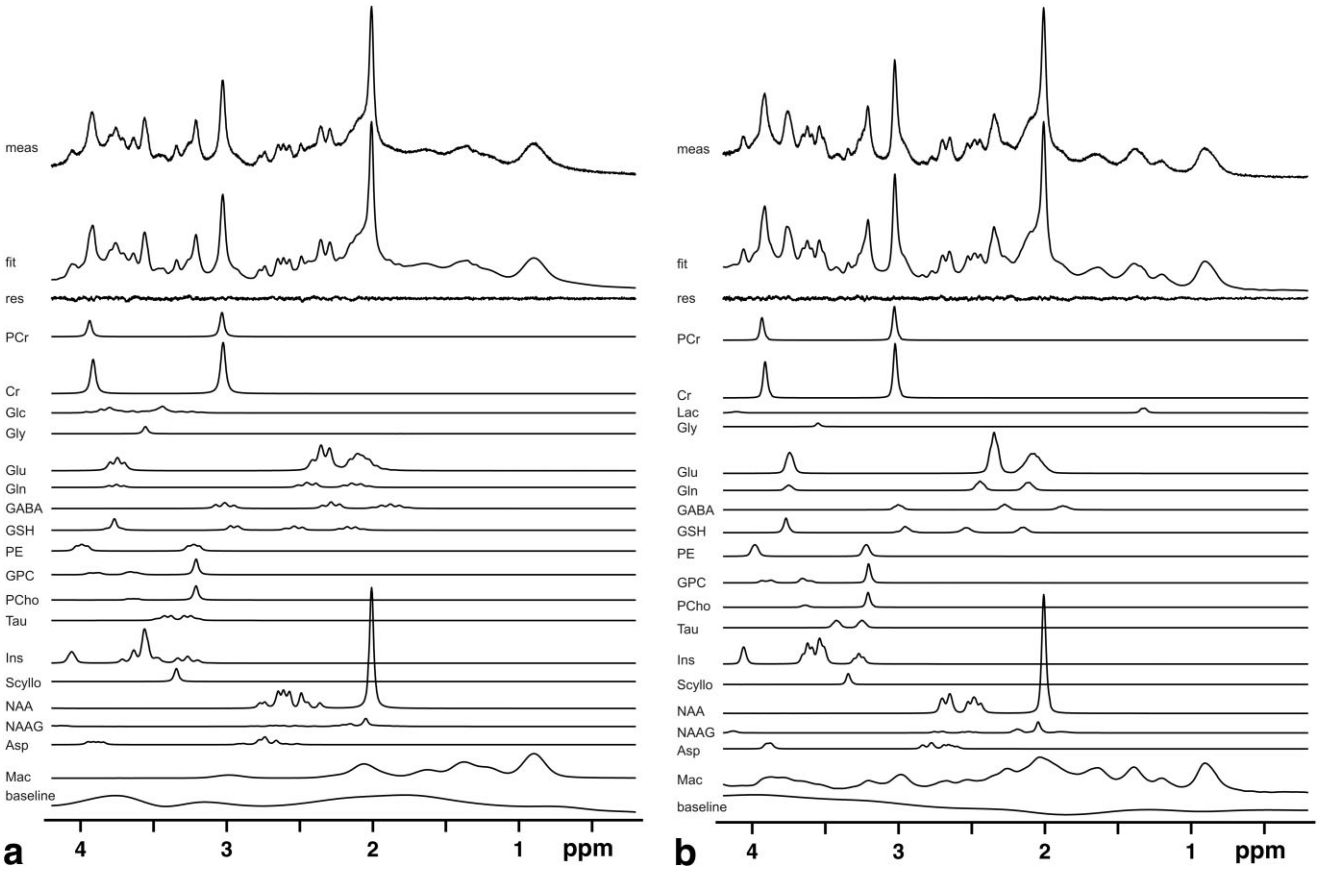

FIG. 5. Fitted curves using LCModel for the human brain spectra acquired at (**a**) 3T (see Fig. 2) and (**b**) 7T (see Fig. 3) for the range of 0.2 to 4.2 ppm. Note the excellent agreement between the data ("meas") and the fit ("fit") also illustrated by the small fit residual ("res") seen below each fit. In addition, LCModel output for metabolite signals (Table 1), macromolecule contributions, and baseline are shown for each spectrum.

Table 1
Metabolite Quantification of ^{1}H Human Brain Spectra Acquired at 3T and 7T*

Metabolite	3T (NA = 128)		7T (NA = 64)	
	Concentration (mmol/kg)	CRLB (%)	Concentration (mmol/kg)	CRLB (%)
Asp	3.1 ± 0.3	7 ± 0.8	2.9 ± 0.5	7 ± 1.3
Cr	5.8 ± 0.2	4 ± 0.5	5.0 ± 0.3	3 ± 0.0
PCr	2.2 ± 0.19	8 ± 0.6	3.0 ± 0.3	5 ± 0.5
GABA	2.5 ± 0.4	8 ± 1.2	1.3 ± 0.15	7 ± 1.0
Gln	1.6 ± 0.4	13 ± 4.4	2.2 ± 0.4	4 ± 1.1
Glu	8.9 ± 0.9	3 ± 0.5	9.9 ± 0.9	1 ± 0.5
GSH	1.4 ± 0.11	6 ± 0.5	1.3 ± 0.2	4 ± 0.5
Ins	5.3 ± 0.6	4 ± 0.5	5.7 ± 0.5	2 ± 0.0
Lac	—	—	0.7 ± 0.1	9 ± 1.6
NAA	11.2 ± 0.8	2 ± 0.5	11.8 ± 0.2	1 ± 0.0
Scyllo	0.4 ± 0.11	8 ± 2.1	0.3 ± 0.12	10 ± 3.9
Tau	1.4 ± 0.5	17 ± 9.9	1.5 ± 0.3	7 ± 2.3
Glc	1.4 ± 0.3	14 ± 2.7	—	—
NAAG	1.0 ± 0.2	11 ± 2.2	1.1 ± 0.4	8 ± 3.8
PE	2.2 ± 0.18	8 ± 0.6	2.5 ± 0.3	5 ± 0.5
GPC+PCho	1.1 ± 0.13	3 ± 0.4	1.1 ± 0.05	3 ± 0.5
NAA+NAAG	12.3 ± 0.9	2 ± 0.4	12.9 ± 0.4	1 ± 0.0
Ins+Gly	6.2 ± 0.6	2 ± 0.4	6.0 ± 0.4	2 ± 0.0
Cr+PCr	8.0 ± 0.3	1 ± 0.5	8.0 ± 0.4	1 ± 0.0
Glu+Gln	10.5 ± 1.2	3 ± 0.0	12.1 ± 1.2	1 ± 0.5

*Absolute concentrations and CRLBs are given as mean values ± SDs for $N = 6$ volunteers (for CRLBs below 20%). For calculating "absolute" concentrations, the value of 8 mmol/kg was considered as the mean concentration of total creatine (tCr = Cr + PCr).
CRLB = Cramér-Rao lower bound.

DISCUSSION

Ultrashort TE spectra of high quality were obtained at 3T and 7T using an optimized implementation of the SPECIAL spectroscopy technique on a clinical platform. Full signal from PRESS and short TEs from STEAM are united in the SE-based SPECIAL method. The adaptation of the pulse sequence for the two field strengths yielded excellent suppression of water signal and lipid contamination. Eddy current postprocessing was not applied, despite the use of gradients of large amplitudes to achieve ultrashort TEs, as no distortion of line shapes was observed. Enhanced localized shimming resulted in improved static magnetic field homogeneity, which is crucial for separating (partially) overlapping resonances and to take advantage of the increased spectral resolution and SNR at higher B_0. The linewidths obtained at 7T in this study were comparable with those previously reported (8), in which an experimental scanner was used. Adapting the implementation of SPECIAL from rat (12) to human brain applications yielded an increase in TE comparable to what was observed with STEAM (8,16). Nevertheless, the advantages of the SPECIAL technique (12) were retained: only one RF refocusing pulse was used, which reduced RF power requirements and improved chemical shift displacement errors. Compared to PRESS, this also makes the sequence less sensitive to B_1 field variations. In addition, signal loss was further minimized by achieving a homogeneous inversion of the magnetization in the selected VOI through the use of an adiabatic inversion pulse, even in the presence of a spatially varying B_1 field. In contrast, imperfect inversion (and/or rapid T_1 relaxation) would lead to signal reduction. Transmitter voltages for RF pulses were on average by a factor of 2.1 higher at 7T compared to 3T, corresponding to a four-fold increase in RF power at the higher field.

It should be noted that volume selection performed with a 1D ISIS approach that is utilized in SPECIAL can be more susceptible to subject motion, frequency shifts (e.g., due to breathing), and possible scanner instability compared to standard single-shot acquisition techniques, such as STEAM and PRESS. On the other hand, in SPECIAL the sensitivity to motion is highly reduced through the application of OVS prior to excitation by nulling the signal from tissues surrounding the VOI. As a consequence, no data degradation due to motion or possible frequency shifts was observed in this study that included the data acquired with the TEM volume coil at 3T (Fig. 4).

In general, using the same RF coil and receiver chain, the SE-based SPECIAL sequence should provide an almost two-fold increase in sensitivity over the STEAM sequence at the same short echo times (12). A reliable quantification of a large number of metabolites at both field strengths was possible, which was attributed to a high SNR in combination with small FWHMs. The observed ratio of the average SNR per unit-time between the two field strengths was 1.7. Considering the almost two-fold (1.97) increase in metabolite FWHM at 7T, this was slightly above the expectation of a linear increase in sensitivity with field strength (21), since the product of 1.7 with 1.97 gives a factor of 3.3, which is somewhat larger than the expected value of 7/3, even when considering experimental error. Deviations from theory are probably due to minor differences in voxel positioning on the two systems in the sensitive volume of the surface coils and to small residual peaks, which are

visible in the "residuals" provided by LCModel (Fig. 5). These peaks do not represent real noise and might differ for simulations with different spectral basis sets at 3T and 7T. Using a spherical doped water phantom and acquiring data for a VOI = 10 × 10 × 10 mm^3 shimmed to 1 Hz linewidth at both field strengths, yielded a ratio of measured SNR of 2.3, which was in line with theoretical predictions. However, other studies reported a supralinear increase in SNR with field strength for a localized volume as well (22).

Despite a reduction in scan time by a factor of two at 7T, the precision of quantification was increased for 12 metabolites using the 7T spectra as judged from the mean CRLB (Table 1), which can be attributed to the increased SNR and spectral resolution at the higher field strength (23). The latter also allowed the improved detection of Lac with CRLB below 20% that is quite remarkable given the low concentration of Lac in the brain under normal conditions (24). The fact that Glc was only quantified at 3T can be explained by its generally complex multiplet pattern collapsing at 3T into two multiplets centered at 3.43 ppm and 3.8 ppm (25) (see Fig. 5a and b), thus somewhat simplifying detection of Glc at this field strength.

In general, metabolite concentrations determined at the two fields were in good agreement. Larger relative differences (>30%) were only observed for PCr, GABA, Gln, and Scyllo, of which, especially GABA, Gln, and Scyllo, are metabolites of low concentration. The quantification of Gln, Tau, and Gln+Glu was clearly more reliable at 7T indicated by the two- to three-fold reduced CRLBs. Similarly, the absolute concentration for GABA measured at 7T (1.3 mmol/kg) approached the literature value of ~1 mmol/kg (25).

The metabolite concentrations determined at 7T (see Table 1) were in good agreement with values reported in (26), where ultrashort TE STEAM data acquired at 7T from VOIs of the same size (8 ml) outside and inside the visual cortex were used for quantification. Different were the concentrations for Asp (different by 66%), myo-Inositol (Ins) (18%), and phosphorylethanolamine (PE) (52%), though CRLBs for these metabolites were slightly (Ins) or substantially (Asp and PE) reduced in the present study. In addition, the estimated concentration of Tau (Table 1) was also found previously (8).

At 3T, only a limited number of studies quantifying a substantial number of metabolites have been reported. Comparing the results presented here to those obtained with SVS (27; Table 4 therein) assuming 8 mM of total creatine (tCr = Cr + PCr), it is noted that concentrations for NAA, NAA+N-acetylaspartylglutamate (NAAG), Glu, Ins, Asp, and Scyllo were in excellent agreement, while concentrations for NAAG, glycerophosphocholine (GPC) + phosphocholine (PCho) = total choline (tCho), glutathione (GSH), PE, and Tau were larger in the previous study (27). However, the number of quantified metabolites was higher in the present study, and the corresponding CRLBs for all of these metabolites were reduced for the 3T results of this study (Table 1) compared to those reported previously (27). Considering the list of metabolite concentrations for GM that were obtained in various 3T and 4T studies (11), it is observed that for tCho, tCr, and NAA the values were in excellent agreement with the 3T results reported here. For Glu and Ins, the results obtained in this study are slightly smaller, though still within the same range of concentrations.

The ability to reliably quantify a large set of metabolites should enhance clinical application of MRS. In this context it is important to note that the use of a TEM volume coil at 3T did not result in significantly reduced data quality (Fig. 4). In particular, the absence of lipid contaminations in the spectrum indicated the effectiveness of the applied OVS scheme. Using a volume coil introduces greater flexibility for examining different anatomical regions. Among the many possible clinical applications include the quantification of GSH, which is believed to be reduced in schizophrenic patients (28), but has been difficult to measure with sufficient precision.

In conclusion, a large number of metabolites can be reliably quantified from single-voxel spectra acquired on clinical scanners in human brain at 3T and 7T using the SPECIAL technique with an echo time on the order of a few milliseconds. The higher SNR and increased spectral resolution at 7T were shown to lead to substantial improvements in precision and accuracy even at a reduced scan time. The proposed localization method features the benefits of ultrashort echo time and high signal intensity and is likely advantageous in situations of RF inhomogeneity and peak RF power limitations such as often encountered at high B_0 fields; e.g., 7T in humans.

REFERENCES

1. Frahm J, Merboldt K-D, Hänicke W. Localized proton spectroscopy using stimulated echoes. J Magn Reson 1987;72:502–508.
2. Bottomley PA. Spatial localization in NMR spectroscopy in vivo. Ann NY Acad Sci 1987;508:333–348.
3. Behar KL, Rothman DL, Spencer DD, Petroff OA. Analysis of macromolecule resonances in 1H NMR spectra of human brain. Magn Reson Med 1994;32:294–302.
4. Seeger U, Klose U, Seitz D, Nagele T, Lutz O, Grodd W. Proton spectroscopy of human brain with very short echo time using high gradient amplitudes. Magn Reson Imaging 1998;16:55–62.
5. Knight-Scott J, Shanbhag DD, Dunham SA. A phase rotation scheme for achieving very short echo times with localized stimulated echo spectroscopy. Magn Reson Imaging 2005;23:871–876.
6. Mlynarik V, Gruber S, Starcuk Z, Starcuk Z Jr, Moser E. Very short echo time proton MR spectroscopy of human brain with a standard transmit/receive surface coil. Magn Reson Med 2000;44:964–967.
7. Tkac I, Gruetter R. Methodology of 1H NMR spectroscopy of the human brain at very high magnetic fields. Appl Magn Reson 2005; 29:139–157.
8. Tkac I, Andersen P, Adriany G, Merkle H, Ugurbil K, Gruetter R. In vivo 1H NMR spectroscopy of the human brain at 7 T. Magn Reson Med 2001;46:451–456.
9. Zhong K, Ernst T. Localized in vivo human 1H MRS at very short echo times. Magn Reson Med 2004;52:898–901.
10. Klomp DW, van der Graaf M, Willemsen MA, van der Meulen YM, Kentgens AP, Heerschap A. Transmit/receive headcoil for optimal 1H MR spectroscopy of the brain in paediatric patients at 3T. MAGMA 2004;17:1–4.
11. Posse S, Otazo R, Caprihan A, Bustillo J, Chen H, Henry PG, Marjanska M, Gasparovic C, Zuo C, Magnotta V, Mueller B, Mullins P, Renshaw P, Ugurbil K, Lim KO, Alger JR. Proton echo-planar spectroscopic imaging of J-coupled resonances in human brain at 3 and 4 Tesla. Magn Reson Med 2007;58:236–244.
12. Mlynarik V, Gambarota G, Frenkel H, Gruetter R. Localized short-echo-time proton MR spectroscopy with full signal-intensity acquisition. Magn Reson Med 2006;56:965–970.
13. Adriany G, Gruetter R. A half-volume coil for efficient proton decoupling in humans at 4 Tesla. J Magn Reson 1997;125:178–184.

14. Vaughan JT, Hetherington HP, Otu JO, Pan JW, Pohost GM. High frequency volume coils for clinical NMR imaging and spectroscopy. Magn Reson Med 1994;32:206–218.
15. Ordidge RJ, Connelly A, Lohman JAB. Image-selected in vivo spectroscopy (ISIS). A new technique for spatially selective NMR spectroscopy. J Magn Reson 1986;66:283–294.
16. Tkac I, Starcuk Z, Choi IY, Gruetter R. In vivo 1H NMR spectroscopy of rat brain at 1 ms echo time. Magn Reson Med 1999;41:649–656.
17. Mao JT, Yan H, Fitzsimmons JR. Slice profile improvement for a clinical MRI system. Magn Reson Imaging 1990;8:767–770.
18. Gruetter R. Automatic, localized in vivo adjustment of all first- and second-order shim coils. Magn Reson Med 1993;29:804–811.
19. Gruetter R, Tkac I. Field mapping without reference scan using asymmetric echo-planar techniques. Magn Reson Med 2000;43:319–323.
20. Provencher SW. Estimation of metabolite concentrations from localized in vivo proton NMR spectra. Magn Reson Med 1993;30:672–679.
21. Hoult DI. Sensitivity and power deposition in a high-field imaging experiment. J Magn Reson Imaging 2000;12:46–67.
22. Ocali O, Atalar E. Ultimate intrinsic signal-to-noise ratio in MRI. Magn Reson Med 1998;39:462–473.
23. Gruetter R, Weisdorf SA, Rajanayagan V, Terpstra M, Merkle H, Truwit CL, Garwood M, Nyberg SL, Ugurbil K. Resolution improvements in in vivo 1H NMR spectra with increased magnetic field strength. J Magn Reson 1998;135:260–264.
24. Barker PB, Lin DDM. In vivo proton MR spectroscopy of the human brain. Prog Nucl Magn Reson Spectrosc 2006;49:99–128.
25. Govindaraju V, Young K, Maudsley AA. Proton NMR chemical shifts and coupling constants for brain metabolites. NMR Biomed 2000;13:129–153.
26. Mangia S, Tkac I, Gruetter R, Van De Moortele PF, Giove F, Maraviglia B, Ugurbil K. Sensitivity of single-voxel 1H-MRS in investigating the metabolism of the activated human visual cortex at 7 T. Magn Reson Imaging 2006;24:343–348.
27. Schulte RF, Boesiger P. ProFit: two-dimensional prior-knowledge fitting of J-resolved spectra. NMR Biomed 2006;19:255–263.
28. Do KQ, Trabesinger AH, Kirsten-Kruger M, Lauer CJ, Dydak U, Hell D, Holsboer F, Boesiger P, Cuenod M. Schizophrenia: glutathione deficit in cerebrospinal fluid and prefrontal cortex in vivo. Eur J Neurosci 2000;12:3721–3728.